

Diamagnetic response of Aharonov-Bohm rings: impurity backward scatterings

Mun Dae Kim,¹ Chul Koo Kim,² and Kyun Nahm³

¹ Korea Institute for Advanced Study, Seoul 130-722, Korea

² Institute of Physics and Applied Physics, Yonsei University, Seoul 120-749, Korea

³ Department of Physics, Yonsei University, Wonju 220-710, Korea

(Dated: February 8, 2020)

We report a theoretical calculation on the persistent currents of disordered normal-metal rings. It is shown that the diamagnetic responses of the rings in the vicinity of the zero magnetic field are attributed to multiple backward scatterings off the impurities. We observe the transition from the paramagnetic response to the diamagnetic one as the strength of disorder grows using both the analytic calculation and the numerical exact diagonalization.

PACS numbers:

I. INTRODUCTION

The phase coherence of electrons in mesoscopic rings gives rise to many interesting quantum phenomena. Among them the persistent current in clean rings induced by the Aharonov-Bohm (AB) flux has been extensively studied and is now well understood both theoretically and experimentally. However, recently, new puzzling behaviors have been observed for the averaged persistent currents in diffusive rings. Experiments clearly indicate that the averaged persistent currents show diamagnetism^{1,2,3,4} in the vicinity of the zero magnetic field in contrary to the existing theory and the amplitude of the persistent current⁵ is much larger than the theoretically predicted values.^{6,7}

There have been several attempts to explain these puzzling behaviors. The repulsive electron-electron interactions may enhance the amplitude of the persistent current, but produce only paramagnetic responses for the ensemble averaged currents.^{8,9} The nonequilibrium ac noise in a mesoscopic ring can cause both the decoherence of electron wave function and the diamagnetic dc current in the loop.¹⁰ Including the spin-orbit scattering in a diffusive ring with ac noise, it was claimed that the sign of persistent current changes from diamagnetic to paramagnetic as the strength of the spin-orbit scattering increases.¹¹ However experiments show that the persistent currents of Au rings² and Ag rings³ with strong spin-orbit interactions as well as of GaAs rings⁴ with a weak one all exhibit the diamagnetic responses. Even though the experiments were performed at much higher temperature than the superconducting transition temperatures, it was claimed that the superconducting fluctuations due to the phonon mediated attractive interaction might lead to a diamagnetic magnetization.¹² Furthermore an attempt which included the large contribution of far levels from the Fermi level¹³ claimed that superconducting fluctuations would give a much larger persistent current.

The magnetic response of an AB ring depends on the parity of the number of electrons n in the ring. For $n = 4N$ the states of the topmost electrons, the clockwise moving and the counterclockwise moving states, are degenerate when AB flux Φ_{ext} is zero. The paramagnetic

current emerges when the degeneracy becomes lifted due to a finite Φ_{ext} and, thus, the circulating direction of the topmost electrons is determined. The ensemble average of the currents of rings with $n = 4N$, $n = 4N \pm 2$ and $n = 4N \pm 1$ show paramagnetic responses with the periodicity $\Phi_0/2$ in clean limit or in weakly disordered case, where $\Phi_0 = h/e$ is the unit flux quantum. However, in a disordered ring, the backward scattering of electrons off the impurities may induce transitions between the two states and thus severely reduce the paramagnetic persistent current for $n = 4N$.

In the disordered systems the backward scattering process occurs through multiple scattering process¹⁴ which leads to rich interesting physical phenomena such as weak localization¹⁵ and universal conductance fluctuation.¹⁶ Experiments for diffusive normal-metal rings¹⁷ as well as wires¹⁸ showed that the resistance oscillation along with the external magnetic field can be explained in terms of the weak localization theory.¹⁹ Therefore we can think that there is much higher backscattering probability in those normal-metal rings. A numerical study showed that the amplitude of backscattering in a disordered multi-channel wire increases along with the length of the wire and the reflection coefficient grows up to become comparable to the transmission coefficient.²⁰

In present study we show that the backscattering process in the diffusive ring induce the transition between the topmost levels and, as a result, the ensemble averaged persistent current changes from paramagnetic to diamagnetic as the impurity strength grows.

II. DIAMAGNETISM DUE TO BACKSCATTERING PROCESS

The Hamiltonian of an AB ring with potential impurity scattering can be given by

$$H = \sum_{k_m} \epsilon_{k_m} c_{k_m}^\dagger c_{k_m} + \sum_{k_m, p} V_p c_{k_m+p}^\dagger c_{k_m}, \quad (1)$$

where $k_m = 2\pi(m + f)/L$ and $p = 2\pi m'/L$ with $f \equiv \Phi_{\text{ext}}/\Phi_0$, the circumference of the ring L and integers m and m' . Here V_p is the Fourier component of the impurity

potential $v(x)$. The scattering term of the Hamiltonian, $\sum_{k_m, p} V_p c_{k_m+p}^\dagger c_{k_m}$, can be divided into the forward scattering and the backscattering process depending on the value of the momentum transfer p . For a diffusive AB ring the forward scattering may reduce the amplitude of persistent current but cannot transfer electrons to oppositely moving states. Thus, although we will consider all the scattering processes in the following exact diagonalization calculation, we first consider only the backward scattering process for transparency of argument.

The backscattering process in an AB ring can be described by $c_{-k_m+q}^\dagger c_{k_m}$, where $q = 2\pi(n + 2f)/L$ with integer n . When there is no threading AB flux and thus $q = 2\pi n/L$, it is sufficient to consider the most dominant process such as $c_{-k_m}^\dagger c_{k_m}$ for $q = 0$ with $n = 0$ at ground state. However, since the value of q cannot be zero for finite AB flux due to the symmetry breaking of the momentum levels, we need to consider the backscattering process with finite q .

For a multichannel wire the backscattering processes take place through multiple scatterings between the states in different channels, which accompany momentum transfer between the initial and the final state. When an electron becomes backscattered eventually, the effective backscattering process can be given by $w(q)c_{-k_m+q}^\dagger c_{k_m}$. If there is no AB flux threading the loop, the effective backscattering can be described as $\omega(q)c_{-k_m}^\dagger c_{k_m}$ approximately with $\omega(q) = \omega_0\delta_{q,0}$. However, for finite Φ_{ext} , $\omega(q)$ will have some distribution which is centered about $q \approx 0$. For example, the backscattering processes between edge states in quantum Hall system through multiple scatterings off impurities show a Lorentzian distribution²¹ and light scatterings from a one-dimensional rough random metal a Gaussian-type distribution for the direction of the reflected waves.²²

Here we take a Gaussian-type distribution for $\omega(q)$

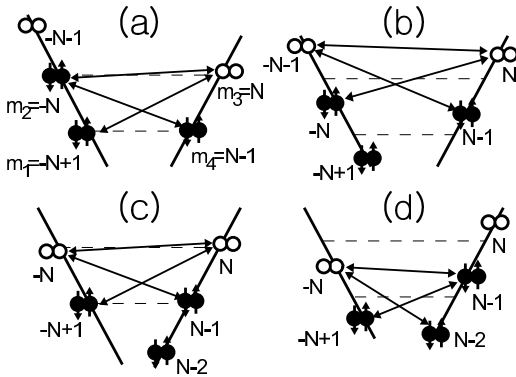


FIG. 1: Energy levels of the AB ring. When $n = 4N$, (a) shows the levels for $f \approx 0$ and (b) for $f \approx 0.5$. (c) and (d) correspond to the case $n = 4N - 2$. Here filled (open) circles denote the occupied (unoccupied) levels.

such as

$$\omega(q) = \omega_0 e^{-\alpha q^2 a^2}, \quad (2)$$

where a is the lattice constant of the loop and we set $\alpha = 0.1$ here and after. Different values of α or different distribution functions result in only quantitatively different behaviors. Then the effective single channel Hamiltonian where the backscattering term comes from multiple scatterings between different channels can be written as follows,

$$H = \sum_{k_m} \epsilon_m c_{k_m}^\dagger c_{k_m} + \sum_{k_m, q} \omega(q) c_{-k_m+q}^\dagger c_{k_m}, \quad (3)$$

where $\epsilon_m \equiv E_0(m + f)^2$ and $E_0 \equiv 2\pi^2 \hbar^2 / m_e L^2$ with the mass of an electron m_e .

Since the scatterings off the impurities occur mainly for the electrons near the Fermi level, it is sufficient to consider the scattering processes between several levels near the Fermi level as shown in Fig. 1. The contribution of other electrons to the persistent current are obtained assuming that they do not participate in the scattering processes.

When an electron is backscattered from the state, $|k_m\rangle$, to the state, $|k_{m'}\rangle$, the scattering matrix element becomes $W_{mm'} \equiv \omega(q)$ with $k_{m'} = -k_m + q$. The Green's function $G_{mm}(\epsilon)$ can be obtained from the equation $(\epsilon \pm is - H)G = I$ which can be written as follows,

$$(\epsilon \pm is - \epsilon_m)G_{mm'}(\epsilon) - \sum_{m'' \neq m} W_{mm''} G_{m''m'}(\epsilon) = \delta_{mm'}. \quad (4)$$

In Fig. 1(a), we consider scatterings between four levels, $m_1 = -N + 1, m_2 = -N, m_3 = N$, and $m_4 = N - 1$, with a small external flux, $f \approx 0$. Including the electrons at the zero momentum state, we can see that the total number of electrons n in Fig. 1(a) is $4N$. The scattering processes are expressed as arrows in Fig. 1(a).

The Green's functions can be obtained from Eq. (4) as follows,

$$G_{m_2 m_2}^{-1}(\epsilon) = \epsilon \pm is - \epsilon_{m_2} - \frac{G_{m_4 m_2}(\epsilon) W_{m_2 m_4} - G_{m_3 m_2}(\epsilon) W_{m_2 m_3}}{G_{m_2 m_2}(\epsilon)}, \quad (5)$$

$$G_{m_4 m_4}^{-1}(\epsilon) = \epsilon \pm is - \epsilon_{m_4} - \frac{W_{m_2 m_4}^2}{\epsilon \pm is - \epsilon_{m_2} - \frac{G_{m_3 m_4}(\epsilon) W_{m_2 m_3}}{G_{m_2 m_4}(\epsilon)}}, \quad (6)$$

where

$$\frac{G_{m_2 m_2}(\epsilon)}{G_{m_2 m_4}(\epsilon)} = \frac{1}{W_{m_2 m_4}} (\epsilon \pm is - \epsilon_{m_4}), \quad (7)$$

$$\frac{G_{m_2 m_4}(\epsilon)}{G_{m_3 m_4}(\epsilon)} = \frac{G_{m_2 m_2}(\epsilon)}{G_{m_2 m_3}(\epsilon)} = \frac{1}{W_{m_2 m_3}} \left[\epsilon \pm is - \epsilon_{m_3} - \frac{W_{m_1 m_3}^2}{(\epsilon \pm is - \epsilon_{m_1})} \right]. \quad (8)$$

The Green's functions $G_{m_3 m_3}(\epsilon)$ and $G_{m_1 m_1}(\epsilon)$ can be obtained from Eqs. (5) and (6) by exchanging the momentum indices; $m_2 \leftrightarrow m_3$ and $m_4 \leftrightarrow m_1$.

All these four Green's functions have the same denominator \mathcal{D} represented as

$$\mathcal{D} = \mathcal{F}_{m_1 m_3} \mathcal{F}_{m_2 m_4} - (\epsilon \pm is - \epsilon_{m_1})(\epsilon \pm is - \epsilon_{m_4}) W_{m_2 m_3}^2 \quad (9)$$

with

$$\mathcal{F}_{m_i m_j} \equiv (\epsilon \pm is - \epsilon_{m_i})(\epsilon \pm is - \epsilon_{m_j}) - W_{m_i m_j}^2, \quad (10)$$

from which we can obtain four poles ϵ^k such that $\epsilon^1 \leq \epsilon^2 \leq \epsilon^3 \leq \epsilon^4$. The persistent currents are calculated using the residues of the Green's functions obtained by $z_{m_i}^k = \lim_{\epsilon \rightarrow \epsilon^k} (\epsilon - \epsilon^k) G_{m_i m_i}(\epsilon)$. Since we consider three scattering particles in four states of Fig. 1(a), the probability that a certain level, m_i , is occupied at the ground state is represented as the sum of the residues of the three lowest energy states, $p_{m_i} = \sum_{k=1}^{n_p} z_{m_i}^k$ with $n_p = 3$.

Since electrons which are not shown in the figure are assumed not to participate in the scattering process, the contributions of these electrons can be obtained simply summing the momentum of each electron,²³

$$I' = -\frac{e}{L} \sum_m \frac{2\pi}{L} (m + f) = -\frac{I_0}{N} \sum_m (m + f) \quad (11)$$

with $I_0 \equiv ev_F/L$ and $v_F \equiv 2\pi N/L$. Therefore, the total persistent current is written as the sum of the two contributions as follows,

$$I = -2\frac{I_0}{N} \left[\sum_{i=1}^4 p_{m_i} (m_i + f) + \sum_{m=m_l}^{m_r} (m + f) \right], \quad (12)$$

where the first part represents the persistent current of the three scattered electrons in Fig. 1(a) and the second one that of the unscattered electrons from $m_l = -N + 2$ to $m_r = N - 2$. The prefactor 2 comes from the spin degeneracy.

When the AB flux f increases to $f \approx 0.5$, the energy levels become shifted as shown in Fig. 1(b). In this case, since the energy levels of the two states, $|N\rangle$ and $|-N-1\rangle$, are much closer than before, the scattering process between these two states becomes important unlike to the case of Fig. 1(a). For the persistent current of Fig. 1(b), we use the definition of parameters; $m_1 = -N + 1, m_2 = -N, m_3 = N, m_4 = N - 1, m_l = -N + 1, m_r = N - 2$ and $n_p = 2$. Here and after we set $N = 100$.

Since we consider a quadratic dispersion, $\epsilon_m = E_0(m + f)^2$, the level spacing at the Fermi level is of the order of NE_0 . Here we define the level spacing $\Delta \equiv NE_0$. In Fig. 2 we show the persistent current I_{4N} for $n = 4N$ with $\omega_0/\Delta = \omega_0/NE_0 = 0.7$ and $\alpha = 0.1$, where the left (right) curve corresponds to Fig. 1(a) (Fig. 1(b)). In the intermediate regime of the external flux f , we extend the results from the both limits to obtain the approximate results as shown in Fig. 2.

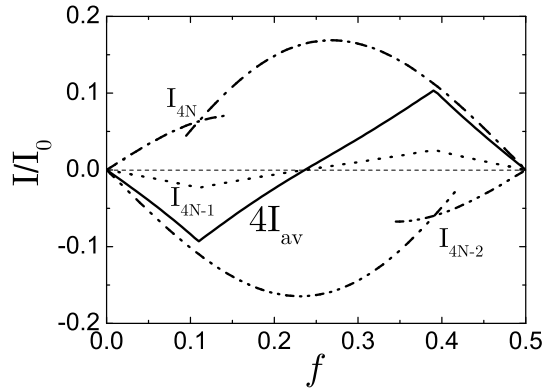


FIG. 2: Persistent currents for $\alpha = 0.1$ and $\omega_0/\Delta = 0.7$. Left (right) curves in I_{4N} and I_{4N-2} correspond to Fig. 1(a) and Fig. 1(c) (Fig. 1(b) and Fig. 1(d)), respectively. We show $4I_{av}$ for the ensemble averaged persistent current instead of I_{av} for clarity.

When the total number of electrons is $n = 4N - 2$, the persistent current I_{4N-2} can also be obtained similarly using the scattering processes shown in Fig. 1(c) and (d), where we use the parameters $m_1 = -N + 1, m_2 = -N, m_3 = N, m_4 = N - 1, m_l = -N + 2, m_r = N - 2$ and $n_p = 2$ for Fig. 1(c) and $m_1 = -N + 1, m_2 = -N, m_3 = N - 1, m_4 = N - 2, m_l = -N + 2, m_r = N - 3$ and $n_p = 3$ for Fig. 1(d).

The dotted line in Fig. 2 shows the persistent current I_{4N-1} for $n = 4N - 1$ which is obtained by the relation $I_{4N-1} = 0.5(I_{4N} + I_{4N-2})$. This relation can be easily understood for clean loops without impurities. If we consider one additional electron at $m = -N$ state in Fig. 1(c), say spin-up electron, it becomes the configuration for $n = 4N - 1$ with the number of spin-up electrons $n_u = 2N$ and spin-down electrons $n_d = 2N - 1$. The configuration for the spin-up electrons is the same as that of Fig. 1(a) with half the number of electrons and, for the spin-down electrons, it corresponds to Fig. 1(c). Since we do not have spin flip processes, the total persistent current is equal to the sum of half the persistent currents of $n = 4N$ and $n = 4N - 2$. In the present case of loops with impurities, if the impurity scattering is not spin dependent so that each spin degree of freedom is decoupled from the other, we have the same relation.

The current I_{4N+1} for $n = 4N + 1$ is the same as that of I_{4N-1} with small difference of $O(1/N)$. Hence, the ensemble averaged persistent current I_{av} can be written as

$$I_{av} = \frac{1}{4}(I_{4N} + I_{4N-2} + 2I_{4N-1}). \quad (13)$$

The ensemble averaged persistent current in clean rings shows the paramagnetic responses for $f \approx 0$, since the paramagnetic currents of I_{4N} dominate over the diamagnetic current I_{4N-2} . Even for an AB loop with impurities, the qualitative picture does not change although

the scattering is expected to reduce the magnitude of the paramagnetic current, if one considers only the forward scatterings off the impurities. However, when we consider contributions from the backward scattering processes, the situation changes drastically as indicated in Fig. 2.

It is well known that the paramagnetic response for $n = 4N$ comes from the contribution of the electrons with $m_2 = -N$ in Fig. 1(a). At $f = 0$ the levels at $m_2 = -N$ and $m_3 = N$ in Fig. 1(a) are degenerate. Finite external flux lifts the degeneracy and the electrons at $m_2 = -N$ contribute a large magnitude of persistent current in addition to the currents by the other electrons in the lower levels, thus resulting in the paramagnetic ensemble averaged current. However, when the backward impurity scattering is sufficiently strong, the impurity scattering causes mixing of the two levels. As a result, the population probability of the level $m_2 = -N$ decreases, whereas that of the level $m_3 = N$ increases. This reduces the paramagnetic I_{4N} and results in the diamagnetic averaged current I_{av} for small f in Fig. 2.

III. NUMERICAL CALCULATION

Since we considered impurity scatterings of only four levels in calculating the Green's functions, the persistent current curves in Fig. 2 are only approximate. In order to obtain more accurate persistent current curves we perform a numerical calculation using the exact diagonalization method, where we include the forward scatterings, $\sum_{k_m, q} w(q) c_{k_m+q}^\dagger c_{k_m}$, as well as the backscatterings. We consider a many-body basis with twelve levels

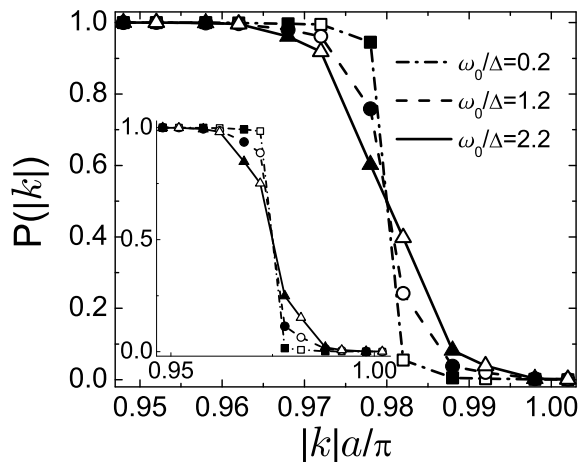


FIG. 3: Momentum distribution of the AB loop for $n = 4N$ with 12 levels of which 7 levels are filled when $f = 0.1$. The horizontal axis denote the absolute value of the wave vector in the loop. The filled (open) marks show the occupation probability of the levels with negative (positive) values of wave vectors. Inset shows the case for $n = 4N - 2$ with 12 levels of which 6 levels are filled.

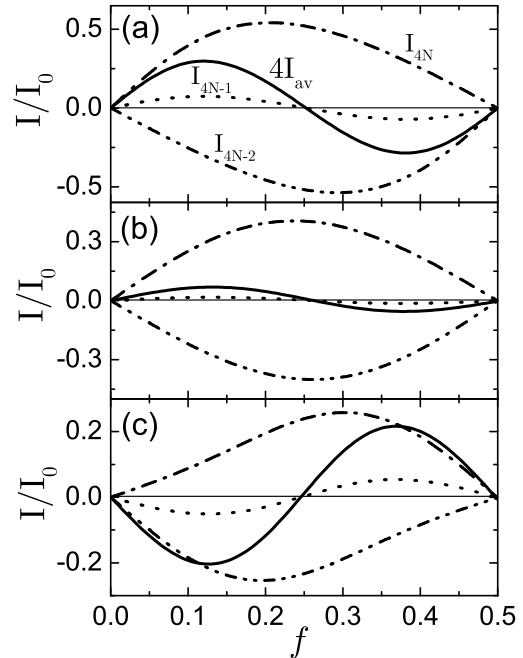


FIG. 4: Persistent currents for (a) $\omega_0/\Delta = 1.2$, (b) $\omega_0/\Delta = 1.6$ and (c) $\omega_0/\Delta = 2.0$ obtained by the exact diagonalization method with 12 levels. I_{4N-1} (the dotted line) is obtained using the relation $I_{4N-1} = 0.5(I_{4N} + I_{4N-2})$.

near the Fermi level, where seven (six) levels are filled for $n = 4N$ ($n = 4N - 2$). If there is no impurity, the ground state is $|111111100000\rangle$ ($|1111111000000\rangle$) in the occupation-number space for $n = 4N$ ($n = 4N - 2$). Here we do not consider spin degree of freedom of electrons and the amplitude of the persistent current will be multiplied by the spin degeneracy at the end of calculation.

We calculate the ground state by diagonalizing the Hamiltonian matrix with 792 (924) basis for several values of ω_0 for $n = 4N$ ($n = 4N - 2$) and show the calculated momentum distribution for $n = 4N$ as a function of the absolute value of momentum level when $f = 0.1$ in Fig. 3. The filled marks denote the levels with negative momentum (left branch) and the open marks with positive momentum (right branch). For weak impurity strength, we note that the lowest seven levels are almost occupied. The seven levels are composed of four levels in the left branch and three levels in the right branch. In this case, it is easily seen that the contribution from the topmost level with $ka/\pi = -0.978$ in left branch becomes dominant.

In Fig. 4(a), we show a paramagnetic persistent current for weak impurity scattering strength $\omega_0/\Delta = 1.2$, where the paramagnetic persistent current I_{4N} dominates over the diamagnetic one I_{4N-2} . Here, the contributions of the electrons which do not participate in the scattering processes to the persistent currents are included as in the second term of Eq. (12). However, as the

strength of the impurity increases, the occupation probability of the topmost level in the left branch decreases while that of the topmost level with $ka/\pi = 0.982$ in the right branch increases as can be seen in Fig. 3. The persistent currents due to these two states cancel each other and only the difference of the population probability $P(|k| = 0.978) - P(|k| = 0.982)$ contributes to the paramagnetic response. In Fig. 3, this corresponds to the difference between the filled mark and the open mark for each value of ω_0 about $ka/\pi \approx 0.98$.

Figure 4(b) shows that the persistent current changes from the paramagnetic to the diamagnetic one as the strength of the impurities increases. When $\omega_0/\Delta = 2.0$ in Fig. 4(c), the difference $P(|k| = 0.978) - P(|k| = 0.982)$ for $n = 4N$ becomes much smaller, whereas it is still very large for $n = 4N - 2$ as shown in the inset of Fig. 3. Therefore, the persistent current I_{4N} becomes weak compared to that of I_{4N-2} and, thus, the ensemble averaged persistent current shows the diamagnetic response as observed in the experiments.^{1,2,3,4} A numerical simulation similar to the previous study²⁰ may be possible. Using

the twisted boundary condition for the wave functions in an AB ring with a disordered zone inserted we think that it can confirm the present results.

IV. SUMMARY

In summary, we have presented a theoretical calculation on the sign of ensemble averaged persistent current for the disordered AB rings. The experimentally observed diamagnetic response is attributed to the transition process of the topmost electrons to the opposite branch for $n = 4N$. It is shown that the backward scatterings of the topmost electrons give rise to the diamagnetic currents in a natural way in agreement with the recent experimental observations.

ACKNOWLEDGMENTS

This work was supported in part by Korea Research Foundation Grant No. KRF-2003-005-C00011.

-
- ¹ L. P. Levy, G. Dolan, J. Dunsmuir, and H. Bouchiat, Phys. Rev. Lett. **64**, 2074 (1990).
² E. M. Q. Jariwala, P. Mohanty, M. B. Ketchen, and R. A. Webb, Phys. Rev. Lett. **86**, 1594 (2001).
³ R. Deblock, R. Bel, B. Reulet, H. Bouchiat, and D. Mailly, Phys. Rev. Lett. **89**, 206803 (2002).
⁴ R. Deblock, Y. Noat, B. Reulet, H. Bouchiat, and D. Mailly, Phys. Rev. B **65**, 075301 (2002).
⁵ V. Chandrasekhar, R. A. Webb, M. J. Brady, M. B. Ketchen, W. J. Gallagher, and A. Kleinsasser, Phys. Rev. Lett. **67**, 3578 (1991).
⁶ H.-F. Cheung, E. K. Riedel, and Y. Gefen, Phys. Rev. Lett. **62**, 587 (1989).
⁷ F. von Oppen and E. K. Riedel, Phys. Rev. Lett. **66**, 84 (1991); B. L. Altshuler, Y. Gefen, and Y. Imry, *ibid.* **66**, 88 (1991).
⁸ V. Ambegaokar and U. Eckern, Phys. Rev. Lett. **65**, 381 (1990); A. Schmid, Phys. Rev. Lett. **66**, 80 (1991); U. Eckern and P. Schwab, Adv. Phys. **44**, 387 (1995).
⁹ A. Müller-Groeling, H. A. Weidenmüller, and C. H. Lewenkopf, Europhys. Lett. **22**, 193(1993); A. Müller-Groeling and H. A. Weidenmüller, Phys. Rev. B. **49**, 4752(1994).
¹⁰ V. E. Kravtsov and V. I. Yudson, Phys. Rev. Lett. **70**, 210 (1993).
¹¹ V. E. Kravtsov and B. L. Altshuler, Phys. Rev. Lett. **84**, 3394 (2000).
¹² V. Ambegaokar and U. Eckern, Europhys. Lett. **13**, 733 (1991).
¹³ M. Schechter, Y. Oreg, Y. Imry, and Y. Levinson, Phys. Rev. Lett. **90**, 026805 (2003).
¹⁴ P. A. Mello, E. Akkermans, and B. Shapiro, Phys. Rev. Lett. **61**, 459 (1988); S. Feng, C. Kane, P. A. Lee, and A. D. Stone, *ibid.*, 834 (1988); A. V. Tartakovski, Phys. Rev. B. **52**, 2704 (1995).
¹⁵ G. Bergmann, Phys. Rep. **107**, 1 (1984); P. A. Lee and T. V. Ramakrishnan, Rev. Mod. Phys. **57**, 287 (1985).
¹⁶ P. A. Lee, A. D. Stone, and H. Fukuyama, Phys. Rev. B **35**, 1039 (1987).
¹⁷ V. Chandrasekhar, M. J. Rooks, S. Wind, and D. E. Prober, Phys. Rev. Lett. **55**, 1610 (1985); C. P. Umbach, C. Van Haesendonck, R. B. Laibowitz, S. Washburn, and R. A. Webb, *ibid.* **56**, 386 (1986); F. P. Milliken, S. Washburn, C. P. Umbach, R. B. Laibowitz, and R. A. Webb, Phys. Rev. B **36**, R4465 (1987); A. G. Aronov and Yu. V. Sharvin, Rev. Mod. Phys. **59**, 755 (1987).
¹⁸ V. Chandrasekhar, P. Santhanam, and D. E. Prober, Phys. Rev. B **44**, 11203 (1991) and references therein.
¹⁹ B. L. Altshuler, A. G. Aronov, and B. Z. Spivak, Pis'ma Zh. Eksp. Teor. Fiz. **33**, 101 (1981) [JETP Lett. **33**, 94 (1981)]; B. L. Altshuler, A. G. Aronov, B. Z. Spivak, D. Yu. Sharin, and Yu. V. Sharin, *ibid.* **35**, 476 (1982) [*ibid.* **35**, 588 (1982)].
²⁰ P. García-Mochales, P. A. Serena, N. García, and J. L. Costa-Krämer, Phys. Rev. B **53**, 10268 (1996).
²¹ S. A. Gurvitz, Phys. Rev. B **51**, 7123 (1995).
²² T. A. Leskova, A. A. Maradudin, and J. Munõz-Lopez, Phys. Rev. E **71**, 036606 (2005).
²³ D. Loss and P. Goldbart, Phys. Rev. B **43**, R13762 (1991); M. D. Kim, S. Y. Cho, C. K. Kim, and K. Nahm, Phys. Rev. B **66**, 193308 (2002).